Signal Processing 89 (2009) 344–351

Contents lists available at ScienceDirect

Signal Processing

journal homepage: www.elsevier.com/locate/sigpro

Fast communication

Fuzzy reasoning-based directional median filter design

Chung-Chia Kang [a], Wen-June Wang [a,b,*]

[a] Department of Electrical Engineering, National Central University, Jhongli, Taoyuan 32001, Taiwan, ROC
[b] Department of Electrical Engineering, National Taipei University of Technology, Taipei 10608, Taiwan, ROC

ARTICLE INFO

Article history:
Received 9 April 2008
Received in revised form
4 September 2008
Accepted 8 September 2008
Available online 21 September 2008

Keywords:
Image processing
Impulse noise
Noise removal
Fuzzy logic
Fuzzy reasoning

ABSTRACT

A novel fuzzy reasoning-based directional median filter is proposed to remove the random-value impulse noise efficiently. In the proposed filter, the differences between the current pixel and the neighbors aligning with four edge directions are applied with fuzzy reasoning technique such that the current pixel is determined as one of three types of pixels: impulse noise pixel, detailed pixel and noise-free pixel. This paper also proposes a simple approach to determine the edge and line direction in the current sliding window while the current pixel is detected as a noise in the detailed region. With the acquired information of the edge direction, the proposed directional median filter can remove the impulse noise and preserve the detail simultaneously. The simulation results show that the proposed filter outperforms several existing filter schemes for impulse noise removal in an image.

1. Introduction

Images are frequently corrupted by impulse noise due to errors generated in noisy sensors and communication channels [1]. The subsequent image processes such as edge detection, image segmentation and object tracking may perform poorly if the input image contains noise. Therefore, detecting noise pixels, and then replacing them with appropriate values, is an important issue in image processing.

Impulse noise distribution can be categorized into two types usually, the types of fixed-value and of random-value [2–7]. In fixed-value impulse noise, a noise pixel takes either a large value 255 or a small value 0. This noise is also called "salt and pepper noise". In random-value impulse noise, the noise value is uniformly distributed in the interval [0,255]. The papers [2–6] have proposed the impulse noise filters only aimed at the fixed-value impulse noise. The above filters outperform any other impulse noise filters no matter these filters are only for random-value impulse noise or for both types of noise. Therefore, this paper only focuses on the random-value impulse noise.

The standard median (MED) filter [1] is a well-known nonlinear filter that eliminates the noise and performs excellently in the smooth region of an image. However, the MED filter might smear the information of edges and lines if the current window is on the detailed region. To solve this problem, the impulse noise filter with detail preservation such as center weighted median (CWM) filter [1], switching median (SWM) filter [8], tri-state median (TSM) filter [9], multi-state median (MSM) filter [10], enhanced rank impulse detector (ERID) [11], differential rank impulse detector (DRID) [11], selective adaptive weighted median filter (SAWMF) [12] and those methods in [13–23] have been proposed to remove the impulse noise and preserve the detail pixels. However, the edge directions of the detail pixels cannot be detected at the same time in the above filters. If the edge directions are acquired by the edge detection methods, such as Canny method [24], competitive fuzzy edge detection (CFED) method [25] and edge detector proposed by Kang and Wang [26] before filtering, then the noise removal performance of the filter will be better than that of the

* Corresponding author at: Department of Electrical Engineering, National Central University, Jhongli, Taoyuan 32001, Taiwan, ROC.
Tel.: +886 3 4227151x34582; fax: +886 3 4255830.
E-mail address: wjwang@ee.ncu.edu.tw (W.-J. Wang).

0165-1684/$ - see front matter © 2008 Elsevier B.V. All rights reserved.
doi:10.1016/j.sigpro.2008.09.003

filter with unknown edge direction. Therefore, Zhang and Karim [27] added four one-dimensional Laplician operators, which are edge detectors, to the SWM filter to enhance its capability of detail preservation. Dong and Xu [28] also combined the functions of edge detection and noise removal together as the directional weighted median (DWM) filter. DWM filter uses the differences between the current pixel and the neighbors aligning with four edge directions to determine whether the current pixel is an impulse noise or not. If yes, the edge direction is determined by a standard deviation-based method, and then the filter works. However, if DWM filter does not have a correct edge direction, the noise removal capability may be reduced (it will be explained in detail in Section 2). Therefore, a new image filter scheme is proposed in this paper to handle this problem.

This paper proposes a fuzzy reasoning-based [29] directional median filter such that the edge and the line direction in the current sliding window are detected correctly and then the noise is removed. The simulations show that the proposed filter has the better noise removal capability than the existing filter schemes.

This paper is organized as follows: Section 2 introduces the directional weighted median filter and the way of threshold selection. Section 3 proposes the fuzzy reasoning-based directional median filter. The simulations and the experimental results are presented in Section 4. Finally, a brief conclusion is given in Section 5.

2. Reviews

Notably, there are two basic assumptions in filtering techniques development. Assumption 1: A noise-free image should be locally smoothly varying and is separated by edges [8]. Assumption 2: A noise pixel takes a gray value substantially larger than or less than those of its neighbors [30]. Here, only the edges aligned with four main directions shown in Fig. 1 are considered. The sliding window $W=\{x_{i-2,j-2},x_{i-2,j-1},\ldots,x_{i+2,j+1},x_{i+2,j+2}\}$ consists of 25 pixels. The current pixel $x_{i,j}$ represents the pixel located on (i,j) in the image. Excluding the current pixel $x_{i,j}$, S_k, $k=1, 2, 3, 4$, denote the other 16 neighbor pixels aligning with four directions, respectively, i.e.

$$S_1=\{x_{i-2,j-2},x_{i-1,j-1},x_{i+1,j+1},x_{i+2,j+2}\}. \tag{1a}$$

$$S_2=\{x_{i,j-2},x_{i,j-1},x_{i,j+1},x_{i,j+2}\}. \tag{1b}$$

$$S_3=\{x_{i+2,j-2},x_{i+1,j-1},x_{i-1,j+1},x_{i-2,j+2}\}. \tag{1c}$$

$$S_4=\{x_{i-2,j},x_{i-1,j},x_{i+1,j},x_{i+2,j}\}. \tag{1d}$$

To determine whether there is any edge or line in the current sliding window, four direction indices are introduced in (2).

$$D_k=\sum_{x\in S_k}|x-x_{i,j}|,\ k=1,2,3,4. \tag{2}$$

In DWM filter, a measurement r is defined as

$$r=\min(D_1,D_2,D_3,D_4). \tag{3}$$

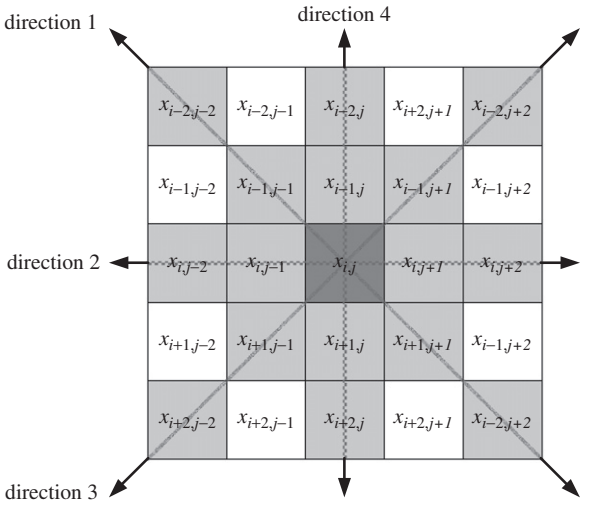

Fig. 1. The current sliding window W and pixels align with four directions.

a

0	0	200	0	0
0	0	200	0	0
0	0	30	0	0
0	0	200	0	0
0	0	200	0	0

b

0	0	200	0	0
0	0	200	0	0
0	0	200	0	0
0	0	30	0	0
0	0	200	0	0

Fig. 2. (a) The case for the current pixel is the impulse noise on the line. (b) The case for the current pixel is on the line and with an impulse noise neighbor.

According to the following three reasons, r is utilized to determine whether the current pixel is a noise pixel.

1. When the current pixel is a noise-free pixel in a smooth region, r is small because of four D_k, $k=1, 2, 3, 4$, are small.
2. When the current pixel is an edge pixel, r is also small because of at least one D_k is small.
3. When the current pixel is an impulse, r is large because of four D_k, $k=1, 2, 3, 4$, are large.

Therefore, the impulse noise detection criterion is presented below. The current pixel $x_{i,j}$ is a noise pixel if $r>T$, where T is a pre-defined threshold. Otherwise, $x_{i,j}$ is noise-free.

However, the above impulse noise detection criterion is only applicable to the following three types of the current pixel, the current pixel is noise-free, an edge pixel, and an impulse noise in the smooth region. Let us consider two cases shown in Fig. 2(a) and (b), the sliding window covers on a line in the smooth region but an impulse noise is on the line. Suppose that the current pixel is an impulse noise pixel in Fig. 2(a), but is a noise-free

pixel in Fig. 2(b). Significantly, the sliding window in Fig. 2(a) appears on the next row of the sliding window in Fig. 2(b). While DWM filter is applied to the sliding windows in Fig. 2(a) and (b), we have r from (3), respectively, as

$$r = \min\{120, 120, 120, 680\} = 120. \tag{4a}$$

$$r = \min\{800, 800, 800, 170\} = 170. \tag{4b}$$

Then to detect the impulse noise in Fig. 2(a) successfully, the threshold T must be set less than 120 via the value r in (4a). However, the current pixel in Fig. 2(b) is detected as an impulse noise and should be removed due to the value $r = 170$ in (4b). Furthermore, DWM filter calculates the standard deviations of gray levels for all pixels belonging to S_k, $k = 1, 2, 3, 4$, respectively, and then takes the minimal one to determine the edge or line direction. In the above illustration, the incorrect edge direction is obtained since the standard deviation of S_4 is the maximal one in Fig. 2(b). Therefore, the noise removal capability of DWM filter is reduced. That means DWM filter has some drawback in the filtering work.

3. Fuzzy reasoning-based directional median filter

In this paper, a fuzzy reasoning-based impulse noise detector is proposed to offer a solution for the issue in Section 2 without setting the threshold T. First, (2) is modified as

$$D_k = \frac{1}{4} \cdot \sum_{x \in S_k} |x - x_{i,j}|, \; k = 1, 2, 3, 4. \tag{5}$$

Then, let the inputs of the fuzzy reasoning be represented as D^l, $l = 1, 2, 3, 4$. The definition of D^l, $l = 1, 2, 3, 4$, is introduced as follows. Sort the direction indices D_k, $k = 1, 2, 3, 4$, in ascending order as $D^1 \leqslant D^2 \leqslant D^3 \leqslant D^4$. The superscript l in D^l, $l = 1, 2, 3, 4$, is the order number of D_k, $k = 1, 2, 3, 4$. Then, let $\Gamma(D^l)$ denote the index k of D_k, $k = 1, 2, 3, 4$, which is at the ascending order l after sorting.

The following five fuzzy rules are used to determine which type of the current pixel should be. The three possible types of the current pixel are impulse noise pixel, detailed pixel and the noise-free pixel.

Rule-1: If D^1 is BIG, D^2 is BIG, D^3 is BIG, and D^4 is BIG, then $x_{i,j}$ is possibly a noise in the smooth region.

Rule-2: If D^1 is SMALL, D^2 is BIG, D^3 is BIG, and D^4 is BIG, then $x_{i,j}$ is an edge pixel.

Rule-3: If D^1 is SMALL, D^2 is SMALL, D^3 is BIG, and D^4 is BIG, then $x_{i,j}$ is possibly a noise in detail.

Rule-4: If D^1 is SMALL, D^2 is SMALL, D^3 is SMALL, and D^4 is BIG, then $x_{i,j}$ is possibly a noise in detail.

Rule-5: If D^1 is SMALL, D^2 is SMALL, D^3 is SMALL, and D^4 is SMALL, then $x_{i,j}$ is a noise-free smooth-region pixel.

BIG(u) and SMALL(u) are fuzzy membership functions shown in (6a) and (6b), respectively. Both are trapezoid shapes and illustrated in Fig. 3.

$$\mathrm{BIG}(u) = \begin{cases} 0, & u < s \\ \frac{u-s}{b-s}, & s \leqslant u < b \\ 1, & u \geqslant b \end{cases}. \tag{6a}$$

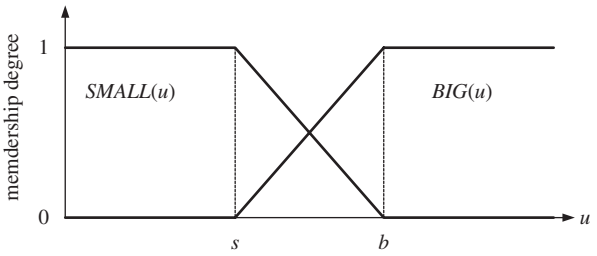

Fig. 3. The trapezoid fuzzy membership functions BIG(u) and SMALL(u).

$$\mathrm{SMALL}(u) = \begin{cases} 1, & u < s \\ \frac{u-b}{s-b}, & s \leqslant u < b \\ 0, & u \geqslant b \end{cases}. \tag{6b}$$

The determination of the two parameters, s and b, depends on the considered image and will be discussed in Section 4. Significantly, the original fuzzy rule base has 16 rules due to four inputs, D^l, $l = 1, 2, 3, 4$, and two fuzzy membership functions, BIG(u) and SMALL(u). To simplify the fuzzy rule base and reduce the computational loading, four inputs have been sorted such that only five fuzzy rules are fired. Let F_m, where m is the rule number, be defined below

$$F_1 = \mathrm{BIG}(D^1) \cdot \mathrm{BIG}(D^2) \cdot \mathrm{BIG}(D^3) \cdot \mathrm{BIG}(D^4). \tag{7a}$$

$$F_2 = \mathrm{SMALL}(D^1) \cdot \mathrm{BIG}(D^2) \cdot \mathrm{BIG}(D^3) \cdot \mathrm{BIG}(D^4). \tag{7b}$$

$$F_3 = \mathrm{SMALL}(D^1) \cdot \mathrm{SMALL}(D^2) \cdot \mathrm{BIG}(D^3) \cdot \mathrm{BIG}(D^4). \tag{7c}$$

$$F_4 = \mathrm{SMALL}(D^1) \cdot \mathrm{SMALL}(D^2) \cdot \mathrm{SMALL}(D^3) \cdot \mathrm{BIG}(D^4). \tag{7d}$$

$$F_5 = \mathrm{SMALL}(D^1) \cdot \mathrm{SMALL}(D^2) \cdot \mathrm{SMALL}(D^3) \cdot \mathrm{SMALL}(D^4). \tag{7e}$$

where the product inference engine [29] is used in (7a)–(7e) to realize the fuzzy reasoning. After all F_m, $m = 1, 2, \ldots, 5$, are obtained, the following cases are processed.

Case-1: If $\max\{F_1, F_2, F_3, F_4, F_5\} = F_1$, the current pixel $x_{i,j}$ is possibly a noise in the smooth region. The standard median filter defined in (8) is directly used to replace it.

$$y_{i,j} = \underset{x \in W}{\mathrm{MED}}\{x\}. \tag{8}$$

Case-2: If $\max\{F_1, F_2, F_3, F_4, F_5\} = F_2$, the current pixel $x_{i,j}$ is an edge pixel and is preserved, $y_{i,j} = x_{i,j}$.

Case-3: If $\max\{F_1, F_2, F_3, F_4, F_5\} = F_3$ or F_4, the current pixel $x_{i,j}$ is possibly a noise in detailed region.

In this case, the directional median filter can be used to remove the noise when the edge direction is obtained. The edge direction is either with direction-$\Gamma(D^1)$ or direction-$\Gamma(D^4)$ because the D^l on the edge direction is obviously different from others. Since D^l, $l = 1, 2, 3, 4$, have been sorted, checking $|D^1 - D^2|$ and $|D^3 - D^4|$ can determine D^1 and D^4 which one is the outlier. If $|D^1 - D^2| \geqslant |D^3 - D^4|$, then D^1 is the outlier, and the impulse noise is on the edge with direction-$\Gamma(D^1)$. Otherwise, D^4 is the outlier, the impulse noise is on the edge with direction-$\Gamma(D^4)$. Let us use the following example shown in Fig. 4 to interpret how the proposed method works in case-3. D_4 is much different

a

150	150	0	150	150
150	150	0	150	150
150	150	50	150	150
150	150	0	150	150
150	150	0	150	150

b

0	0	150	0	0
0	0	150	0	0
0	0	50	0	0
0	0	150	0	0
0	0	150	0	0

c

150	150	0	0	0
150	150	0	0	0
150	150	50	0	0
150	150	0	0	0
150	150	0	0	0

d

150	150	150	0	0
150	150	150	0	0
150	150	50	0	0
150	150	150	0	0
150	150	150	0	0

Fig. 4. Four cases for the current pixel is the impulse noise on the line and edge.

from the other three direction indices despite D_4 is the minimal ($D^1 = D_4 = 50$, $D_1 = D_2 = D_3 = 100$ in Fig. 4(a)) or the maximal one ($D^4 = D_4 = 100$, $D_1 = D_2 = D_3 = 50$ in Fig. 4(b)). Similar consideration is also shown in Fig. 4(c) and (d). In Fig. 4(c), $D^1 = D_4 = 50$ and $D_1 = D_2 = D_3 = 75$. In Fig. 4(d), $D^4 = D_4 = 100$, $D_1 = D_2 = D_3 = 75$. Since the direction of the edge is obtained, the directional median filter can be used to remove the impulse noise. The directional median filter is re-defined as

$$y_{i,j} = \begin{cases} \underset{x \in S_{\Gamma(D^1)}}{\text{MED}} \{x_{i,j}, x\}, \text{if} |D^1 - D^2| \geqslant |D^3 - D^4| \\ \underset{x \in S_{\Gamma(D^4)}}{\text{MED}} \{x_{i,j}, x\}, \text{if} |D^1 - D^2| < |D^3 - D^4| \end{cases}. \quad (9)$$

Case-4: If $\max\{F_1, F_2, F_3, F_4, F_5\} = F_5$, the current pixel $x_{i,j}$ is a noise-free pixel in a smooth region and should be preserved, $y_{i,j} = x_{i,j}$.

4. Simulations and results

The values of parameters s and b in the fuzzy membership functions must be set in advance. The well-known "Lena", "building", "baboon" and "peppers" images were adopted as the test images with 40% random-value impulse noise. "Lena" and "peppers" images are smooth images, while "building" and "baboon" are complicated images. Both "Lena" and "baboon" are with 512×512 size, while both "building" and "peppers" are with 256×256 size. The peak signal-to-noise ratio (PSNR) [1] and the mean absolute error (MAE) [1] between the restored image and the original image were selected as the performance index. The PSNR and MAE are defined as (10) and (11), respectively.

$$\text{PSNR} = 10 \cdot \log \frac{255^2}{(1/I \cdot J) \sum_{i=1}^{I} \sum_{j=1}^{J} (y_{i,j} - s_{i,j})}. \quad (10)$$

$$\text{MAE} = \frac{1}{I \cdot J} \sum_{i=1}^{I} \sum_{j=1}^{J} |y_{i,j} - s_{i,j}| \quad (11)$$

where $I \times J$ is the image size; $y_{i,j}$ and $s_{i,j}$ are the restored and original pixels, respectively, on the location (i,j) in the image. Calculate PSNR for four images and take the average value of PSNR for four simulations as the total performance. By tries and errors, the better performance occurs with the parameters $s \in [10,30]$ and $b \in [60,80]$. When the parameters are in these intervals, the proposed method outperforms other methods, especially, there is the best performance at $s = 20$ and $b = 70$. Therefore, $s = 20$ and $b = 70$ were chosen as the suggested parameters in the fuzzy membership functions of the proposed method. Fig. 5 shows the noise removal capability of the proposed method when $s \in [10,30]$ and $b \in [60,80]$.

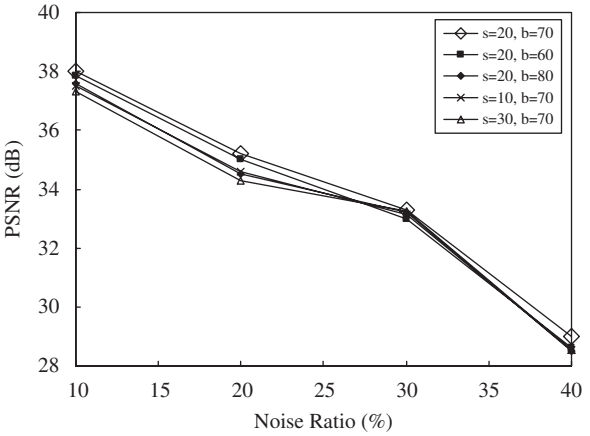

Fig. 5. Test for different parameters s and b of the fuzzy membership functions.

To test the noise removal capability of the proposed impulse noise filter, the simulation results were compared with the results by the filters such as MED [1], CWM [1], SWM [8], TSM [9], MSM [10], ERID [11], DRID [11], SAWMF [12], the method proposed by Chen and Wu [13], the method proposed by Zhang and Karim [27], and DWM [28]. Tables 1–3 list the PSNR and MAE values of restored images with random-value impulse noise $p = 0\%$, 5%, 10%, 20%, 30%, and 40% for "Lena", "building", "bridge" and "camera-man" images, respectively. The proposed method achieved the best PSNRs when $p = 5$–40%.

Fig. 6 shows the corrupted "Lena" image with $p = 20\%$ random-value impulse noise and the corresponding restored images filtered by MED, TSM, MSM, ERID, DRID, SAWMF, the method proposed by Chen and Wu, the

Table 1
PSNRs (MAEs) results with $p = 0\%$ and 5% random-value impulse noise

Method	$p = 0\%$				$p = 5\%$			
	Lena	Building	Bridge	Camera-man	Lena	Building	Bridge	Camera-man
Noisy images	∞ (0)	∞ (0)	∞ (0)	∞ (0)	22.32 (3.59)	21.86 (3.74)	22.24 (3.62)	22.51 (3.56)
MED	42.09 (0.82)	33.11 (2.07)	30.58 (3.41)	32.42 (2.86)	39.11 (1.04)	31.67 (2.65)	28.68 (3.72)	30.43 (3.04)
CWM	43.64 (0.49)	32.33 (2.15)	29.97 (3.23)	33.11 (2.61)	39.67 (0.98)	31.54 (2.31)	28.81 (2.80)	30.84 (2.13)
SWM-I	**66.61 (0.00)**	33.41 (1.21)	33.22 (0.78)	35.21 **(0.33)**	39.49 (0.60)	31.89 (1.55)	29.27 (2.42)	30.86 (1.85)
SWM-II	54.72 (0.01)	30.61 (3.14)	30.21 (4.03)	32.62 (3.03)	37.62 (0.93)	30.64 (3.65)	28.12 (3.84)	29.99 (2.98)
TSM	49.87 (0.03)	35.40 **(0.67)**	31.32 (1.92)	33.45 (1.74)	40.82 (0.33)	33.38 **(0.80)**	30.12 (2.23)	31.58 (2.10)
MSM	46.14 (0.13)	33.17 (1.93)	30.66 (2.81)	33.03 (2.16)	39.25 (0.91)	32.61 (1.62)	29.75 (2.96)	31.29 (2.75)
ERID	45.18 (0.09)	33.32 (0.99)	29.92 (2.49)	32.42 (2.16)	40.56 (0.31)	31.82 (1.58)	29.05 (2.95)	30.77 (2.47)
DRID	46.43 (0.26)	32.77 (1.34)	29.12 (3.47)	30.93 (3.72)	37.73 (1.75)	30.73 (2.30)	27.88 (3.64)	29.97 (3.17)
SAWMF	53.18 (0.01)	32.91 (1.97)	31.26 (2.82)	33.65 (2.46)	39.86 (0.77)	31.87 (2.69)	29.09 (3.01)	31.48 (2.20)
Chen and Wu	53.16 (0.01)	33.37 (1.60)	32.00 (1.88)	33.73 (1.99)	40.59 (0.39)	32.61 (1.63)	29.29 (2.27)	31.29 (1.86)
Zhang and Karim	56.94 (0.01)	31.65 (2.18)	31.31 (2.10)	33.85 (1.59)	39.67 (0.71)	31.34 (2.05)	28.62 (2.75)	31.21 (2.56)
DWM	57.85 (0.01)	33.09 (1.51)	33.01 (1.07)	35.45 (0.64)	40.30 (0.31)	32.86 (0.99)	29.76 (1.73)	31.76 (1.58)
Ours	58.79 (0.01)	**33.63 (0.93)**	**33.39 (0.69)**	**35.56** (0.35)	**41.88 (0.28)**	**33.76 (0.96)**	30.65 **(1.56)**	**32.52 (1.44)**

Table 2
PSNRs (MAEs) results with $p = 10\%$ and 20% random-value impulse noise

Method	$p = 10\%$				$p = 20\%$			
	Lena	Building	Bridge	Camera-man	Lena	Building	Bridge	Camera-man
Noisy images	19.38 (7.13)	18.75 (7.63)	19.18 (7.33)	19.41 (7.17)	16.21 (14.67)	15.72 (15.49)	16.16 (14.74)	16.44 (14.35)
MED	33.63 (1.64)	30.01 (3.91)	28.31 (3.41)	31.54 (2.15)	28.12 (2.90)	27.82 (4.14)	26.13 (5.22)	29.50 (4.27)
CWM	33.65 (1.33)	31.55 (2.67)	29.63 (2.67)	32.16 (1.67)	28.78 (3.47)	27.68 (4.39)	26.33 (5.42)	29.59 (4.23)
SWM-I	32.33 (1.24)	31.08 (3.33)	29.09 (2.60)	32.11 **(1.25)**	28.91 (3.51)	28.41 (4.46)	26.61 (4.79)	28.97 (3.23)
SWM-II	30.94 (2.31)	29.95 (5.51)	28.81 (3.82)	32.31 (1.48)	25.86 (4.67)	23.95 (5.81)	23.70 (6.97)	26.66 (5.56)
TSM	38.13 (0.46)	33.58 (2.64)	29.97 (2.70)	32.23 (1.69)	32.97 (2.01)	30.95 (3.71)	28.11 (4.16)	30.61 (2.78)
MSM	35.72 (0.95)	32.34 (2.97)	28.43 (3.31)	31.01 (2.29)	32.94 (2.63)	30.26 (3.16)	27.02 (3.88)	29.20 (3.08)
ERID	35.74 (0.82)	31.93 (2.61)	28.85 (3.34)	31.46 (2.40)	29.44 (2.46)	27.58 (4.63)	25.90 (4.98)	29.69 (3.38)
DRID	33.53 (1.93)	29.36 (3.62)	27.85 (4.14)	31.40 (3.15)	27.48 (3.94)	26.32 (5.40)	25.31 (5.55)	28.24 (4.03)
SAWMF	36.47 (1.31)	34.18 (2.58)	30.35 (3.73)	31.78 (3.11)	32.51 (2.60)	28.85 (3.57)	26.74 (4.76)	28.88 (4.36)
Chen and Wu	36.88 (1.36)	32.93 (2.31)	29.08 (3.98)	31.44 (3.30)	33.31 (2.16)	29.62 (3.94)	26.92 (5.06)	30.64 (4.17)
Zhang and Karim	36.30 (0.98)	32.30 (2.08)	29.49 (3.02)	31.85 (2.60)	31.12 (2.54)	30.06 (2.66)	27.54 (3.81)	29.65 (3.41)
DWM	38.04 (0.62)	35.15 (1.65)	31.25 (2.64)	32.65 (2.25)	35.06 (1.64)	31.32 (2.64)	28.32 (3.43)	31.02 (2.62)
Ours	**38.83 (0.31)**	35.62 **(1.41)**	32.18 **(2.02)**	**33.91** (1.66)	**36.33 (1.23)**	32.84 **(1.96)**	29.67 **(2.93)**	**31.96 (2.37)**

Table 3
PSNRs (MAEs) results with $p = 30\%$ and 40% random-value impulse noise

Method	$p = 30\%$				$p = 40\%$			
	Lena	Building	Bridge	Camera-man	Lena	Building	Bridge	Camera-man
Noisy images	14.51 (21.76)	14.06 (22.72)	14.46 (21.88)	14.64 (21.56)	13.22 (29.17)	12.68 (30.92)	13.15 (29.47)	13.43 (28.52)
MED	28.77 (3.94)	26.65 (6.27)	24.77 (7.44)	26.12 (5.96)	24.94 (6.28)	22.46 (8.65)	21.33 (9.03)	23.35 (6.95)
CWM	25.90 (4.52)	25.03 (6.41)	24.05 (7.02)	25.85 (5.79)	22.37 (7.96)	22.04 (9.03)	21.55 (9.07)	22.61 (8.01)
SWM-I	25.62 (4.86)	24.89 (6.28)	23.83 (6.79)	25.71 (5.37)	22.84 (8.61)	22.64 **(7.15)**	21.99 (8.33)	23.32 (7.90)
SWM-II	23.56 (4.91)	22.37 (8.64)	21.25 (8.97)	24.60 (6.42)	21.73 (8.68)	21.43 (9.66)	19.48 (10.65)	21.33 (7.74)
TSM	27.78 (2.83)	26.58 **(5.14)**	25.05 **(6.24)**	26.85 (4.84)	23.91 (6.32)	23.49 (8.48)	22.58 (8.61)	24.49 (5.98)
MSM	25.31 (3.64)	22.95 (7.69)	22.70 (7.57)	25.03 (5.30)	22.86 (6.34)	21.63 (8.40)	21.46 (8.42)	23.71 (6.35)
ERID	24.53 (3.68)	23.64 (7.45)	23.08 (7.70)	25.09 (5.57)	21.24 (7.91)	20.61 (8.62)	20.53 (9.12)	22.68 (6.78)
DRID	23.12 (4.49)	22.43 (7.51)	22.08 (7.67)	24.54 (6.22)	20.28 (9.76)	20.16 (8.34)	19.93 (9.36)	21.62 (7.67)
SAWMF	26.32 (3.64)	24.57 (5.94)	22.95 (7.30)	25.89 (5.56)	23.96 (6.82)	21.95 (8.31)	20.63 (8.72)	21.97 (7.44)
Chen and Wu	28.13 (2.84)	25.76 (6.73)	24.45 (7.53)	27.55 (5.65)	24.75 (7.49)	24.15 (7.65)	22.88 (8.38)	25.04 (6.18)
Zhang and Karim	24.95 (4.65)	23.21 (7.16)	23.02 (7.61)	25.20 (5.82)	22.15 (8.62)	22.04 (8.10)	21.39 (8.65)	22.76 (6.95)
DWM	30.14 (2.15)	26.83 (6.65)	25.67 (6.90)	29.07 (4.16)	28.44 (4.56)	25.01 (7.37)	23.62 **(7.56)**	26.20 (4.74)
Ours	**31.65 (1.51)**	**27.87 (6.08)**	**26.83** (6.26)	**30.22 (3.75)**	**29.37 (4.44)**	**25.79 (7.31)**	**24.59** (7.64)	**27.39 (4.69)**

method proposed by Zhang and Karim, DWM and the proposed method, respectively. Fig. 7 shows the corrupted "building" image with $p = 40\%$ random-value impulse noise and the corresponding restored images. The threshold value T, and/or other parameters w and s were the best values recommended in the literatures or tried by us.

Fig. 8 shows the mean PSNR values against the noise ratio p within [10%,60%] by nine filters for nine test

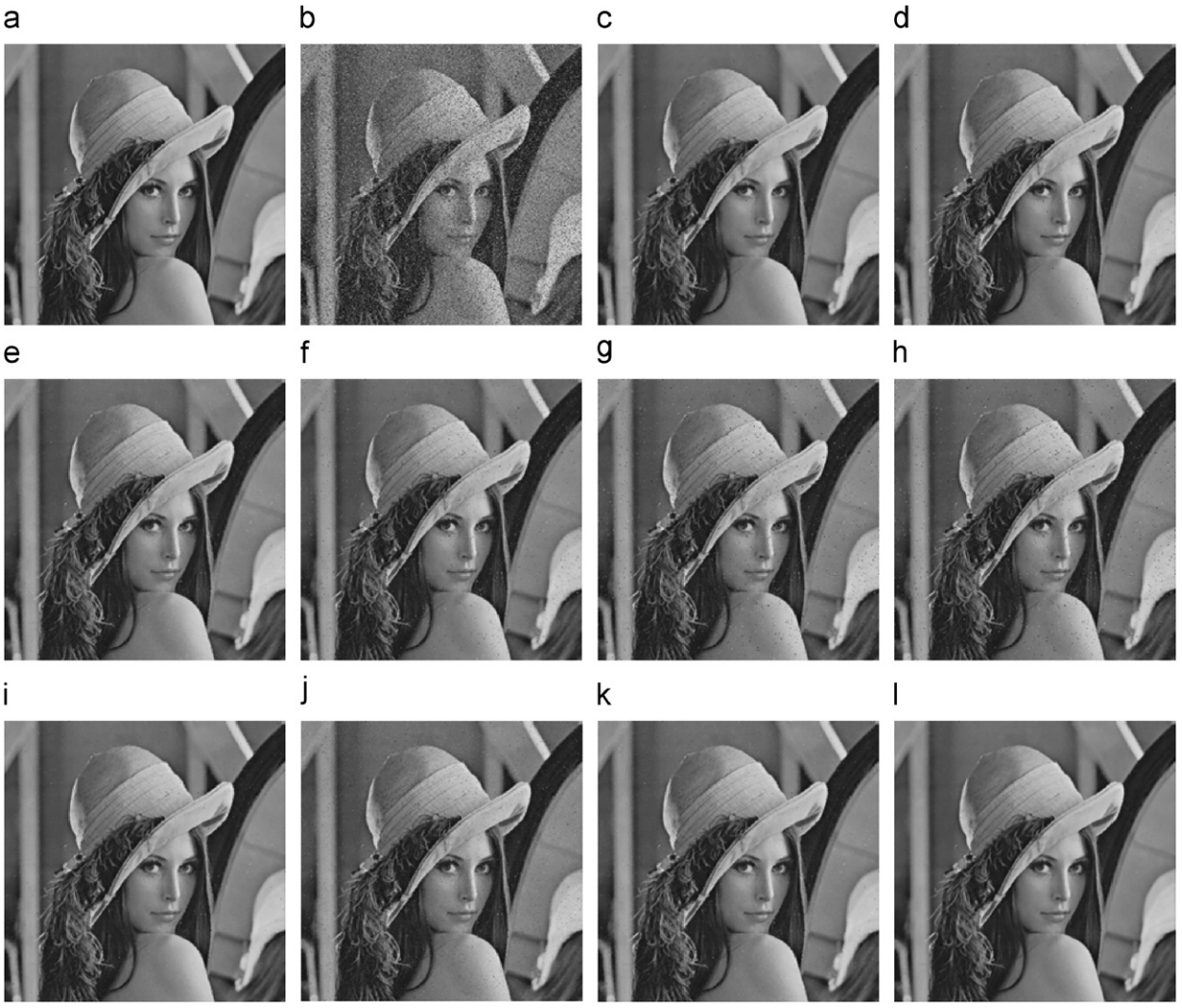

Fig. 6. (a) The original "Lena" image; (b) The corrupted "Lena" with 20% random-value impulse noise; (c) MED; (d) TSM; (e) MSM; (f) ERID; (g) DRID; (h) SAWMF; (i) Chen and Wu; (j) Zhang and Karim; (k) DWM and (l) the proposed method.

images, "Lena", "building", "baboon", "peppers", "bridge", "camera-man", "airplane", "boat" and "house", corrupted by the random-value impulse noise. The higher the noise ratio produced, the lower the PSNR is in the corresponding restored image. The proposed method achieved the image quality with the best PSNR values.

5. Conclusion

Notably, if DWM filter does not have a correct edge direction, the noise removal capability may be reduced. Therefore, a direction median filter based on fuzzy reasoning has been proposed to handle this problem. Similar to DWM filter, the differences between the current pixel and the neighbors aligning with four edge directions are adopted first. However, the current pixel is determined as an impulse noise, detailed pixel or the noise-free pixel via the simple computation in the fuzzy reasoning. If the current pixel is detected as a detailed pixel or a noise-free pixel, then it can be preserved. If the current pixel is detected as an impulse noise in the smooth region, then the standard median filter is used to remove it. While the current pixel is detected as an impulse noise in the detailed region, this paper furthermore proposes a simple approach to determine the edge or line direction of the current sliding window. With the acquired information of the edge direction, the proposed directional median filter can remove the impulse noise and preserve the detail simultaneously. However, the arbitrary directions of edge may not be detected because only four directions of edge are considered in the overwhelming majority of edge detection methods and detail preserving filters including DWM and the proposed filter. Therefore, we cannot guarantee that the arbitrary directions of edge can be preserved in the proposed method.

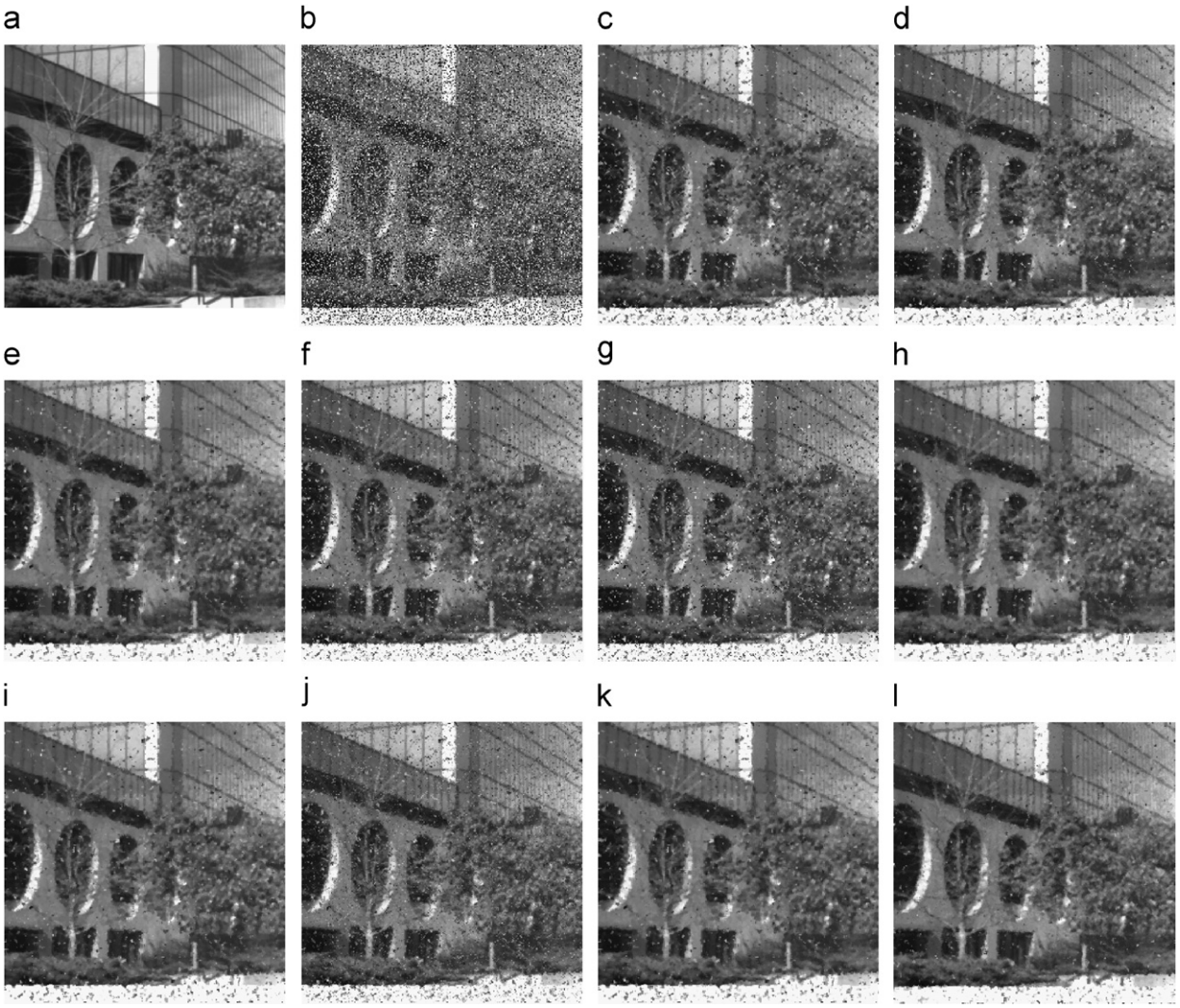

Fig. 7. (a) The original "building" image; (b) The corrupted "building" with 40% random-value impulse noise; (c) MED; (d) TSM; (e) MSM; (f) ERID; (g) DRID; (h) SAWMF; (i) Chen and Wu; (j) Zhang and Karim; (k) DWM and (l) the proposed method.

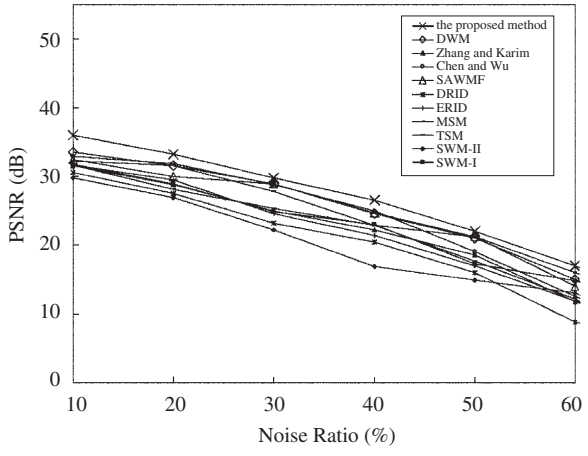

Fig. 8. Mean PSNRs against the noise ratios of nine filters for nine test images.

Acknowledgements

The authors would like to thank the National Science Council of the Republic of China, Taiwan for financially supporting this research under Contract No. NSC-96-2221-E-027-136.

References

[1] R.C. Gonzalez, R.E. Woods, Digital Image Processing, Addison-Wesley, New York, 1992.
[2] Z. Wang, D. Zhang, Progressive switching median filter for the removal of impulse noise from highly corrupted images, IEEE Trans. Circuits Syst. II, Analog Digit. Signal Process. 46 (1) (1999) 78–80.
[3] G. Pok, J.C. Liu, A.S. Nair, Selective removal of impulse noise based on homogeneity level information, IEEE Trans. Image Process. 12 (1) (2003) 85–92.
[4] W. Luo, Efficient removal of impulse noise from digital images, IEEE Trans. Consum. Electron. 52 (2) (2006) 523–527.
[5] P.E. Ng, K.K. Ma, A switching median filter with boundary discriminative noise detection for extremely corrupted images, IEEE Trans. Image Process. 15 (6) (2006) 1506–1516.

[6] T.C. Chiang, C.H. Chiu, W.J. Wang, A fuzzy rule based adaptive center weighted median filter, Int. J. Comput. Appl. Technol. 27 (2/3) (2006) 192–203.
[7] J.Y. Chang, J.L. Chen, Classifier-augmented median filters for image restoration, IEEE Trans. Instrum. Meas. 53 (2) (2004) 351–356.
[8] T. Sun, Y. Neuvo, Detail-preserving median based filters in image processing, Pattern Recognit. Lett. 15 (1994) 341–347.
[9] T. Chen, K.K. Ma, L.H. Chen, Tri-state median for image denoising, IEEE Trans. Image Process. 8 (12) (1999) 1834–1838.
[10] T. Chen, H.R. Wu, Space variant median filters for the restoration of impulse noise corrupted images, IEEE Trans. Circuits Syst. II, Analog Digit. Signal Process. 48 (8) (2001) 784–789.
[11] I. Aizenberg, C. Butakoff, Effective impulse detector based on rank-order criteria, IEEE Signal Process. Lett. 11 (3) (2004) 363–366.
[12] L. Jin, C. Xiong, D. Li, Selective adaptive weighted median filter, Opt. Eng. 47 (3) (2008) 1–5.
[13] T. Chen, H.R. Wu, Adaptive impulse detection using center-weighted median filters, IEEE Signal Process. Lett. 8 (1) (2001) 1–3.
[14] W. Luo, A new efficient impulse detection algorithm for the removal of impulse noise, IEICE Trans. Fundam. Electron. Commun. Comput. Sci. E 88-A (10) (2005) 2579–2586.
[15] W. Luo, A new impulse detector based on order statistics, AEÜ Int. J. Electron. Commun. 60 (6) (2006) 462–466.
[16] H.L. Eng, K.K. Ma, Noise adaptive soft-switching median filter, IEEE Trans. Image Process. 10 (2) (2001) 242–251.
[17] L. Jin, D. Li, A switching vector median filter based on the CEILAB color space for color image restoration, Signal Process. 87 (6) (2007) 1345–1354.
[18] A. Toprak, I. Guler, Impulse noise reduction in medical images with the use of switch mode fuzzy adaptive median filter, Digit. Signal Process. 17 (4) (2007) 711–723.
[19] V. Zlokolica, M. De Geyter, S. Schulte, A. Pizurica, W. Philips, E.E. Kerre, Fuzzy logic recursive change detection for tracking and denoising of video sequences, in: Proceedings of Image and Video Communications and Processing 2005 (SPIE), San Jose, CA, USA, January 2005, pp. 771–782.
[20] V. Zlokolica, W. Philips, D. Van De Ville, A new non-linear filter for video processing, in: Proceedings of the Third IEEE Benelux Signal Processing Symposium, Leuven, Belgium, March 2002, pp. 221–224.
[21] S. Schulte, S. Morillas, V. Gregori, E. Kerre, A new fuzzy color correlated impulse noise reduction method, IEEE Trans. Image Process. 16 (10) (2007) 2565–2575.
[22] A. Rosales-Silva, V.I. Ponomaryov, F.J. Gallegos-Funes, Fuzzy vector directional filters for multichannel image denoising, Lect. Notes Comput. Sci. 4756 (2007) 124–133.
[23] S. Schulte, V. De Witte, M. Nachtegael, D. Van der Weken, E.E. Kerre, Fuzzy two-step filter for impulse noise reduction from color images, IEEE Trans. Image Process. 15 (11) (2006) 3568–3579.
[24] J.F. Canny, A computational approach to edge detection, IEEE Trans. Pattern Anal. Mach. Intell. 8 (1986) 679–698.
[25] L.R. Liang, C.G. Looney, Competitive fuzzy edge detection, Appl. Soft Comput. J. 3 (2) (2003) 123–137.
[26] C.C. Kang, W.J. Wang, A novel edge detection method based on the maximizing objective function, Pattern Recognit. 40 (2) (2007) 609–618.
[27] S. Zhang, M.A. Karim, A new impulse detector for switching median filters, IEEE Signal Process. Lett. 9 (11) (2002) 360–363.
[28] Y. Dong, S. Xu, A new directional weighted median filter for removal of random-valued impulse noise, IEEE Signal Process. Lett. 14 (3) (2007) 193–196.
[29] L.X. Wang, Adaptive Fuzzy Systems and Control: Design and Stability Analysis, Prentice-Hall, Englewood Cliffs, NJ, 1994.
[30] D. Zhang, Z. Wang, Impulse noise removal using polynomial approximation, Opt. Eng. 37 (4) (1998) 1275–1282.